Available online at www.sciencedirect.com

ScienceDirect

Solid Earth Sciences 2 (2017) 109–122

www.elsevier.com/locate/SESCI

Re–Os isotope geochronology of the Shangbao pyrite–flourite deposit in southeastern Hunan, South China: Evidence for multiple mineralization events and the role of crust–mantle interaction in polymetallic deposits

Cheng-Cheng Huang [a,b], Hai-Feng Guo [a], Jie Li [a], Qiang Wang [a,b,c,*], Chunfu Zhang [d], Derek Wyman [e], Gong-Jian Tang [a]

[a] *State Key Laboratory of Isotope Geochemistry, Guangzhou Institute of Geochemistry, Chinese Academy of Sciences, Guangzhou 510640, China*
[b] *University of Chinese Academy of Sciences, Beijing 10069, China*
[c] *CAS Center for Excellence in Tibetan Plateau Earth Sciences, Beijing 100101, China*
[d] *Department of Geosciences, Fort Hays State University, Hays, KS 67601-4099, USA*
[e] *School of Geosciences, University of Sydney, NSW 2006, Australia*

Received 24 March 2017; revised 12 April 2017; accepted 12 April 2017
Available online 1 June 2017

Abstract

In South China, both crustal reworking and crust–mantle interaction were important geological processes during the Paleozoic and Mesozoic eras. However, the relationships between these two processes and metal mineralization are still unknown. Here we report rhenium and osmium isotopic data for pyrite grains from a pyrite deposit associated with a granite intrusion in the Shangbao area, southeastern Hunan Province (South China). Two pyrite samples, both containing many euhedral pyrite grains, were collected from the same locality, but the samples yield distinct ages. Six euhedral pyrite grains from one sample yield an isochronal age of 279 ± 12 Ma, with an initial $^{187}Os/^{188}Os$ ratio of 0.39 ± 0.71, and Re and Os concentrations of 0.12–63.5 ppb and 2.14–185 ppt, respectively. This Early Permian age is in good agreement with the age of the strata that host the pyrite deposit. Five euhedral pyrite grains from the other sample yield an isochronal age of 75.2 ± 4.3 Ma, with an initial $^{187}Os/^{188}Os$ ratio of 0.141 ± 0.030 and Re and Os concentrations of 0.15–0.43 ppb and 1.0–39.9 ppt, respectively. If one pyrite grain with the highest $^{187}Re/^{188}Os$ and $^{187}Os/^{188}Os$ ratios is excluded, other four pyrite grains give an isochronal age of 85 ± 13 Ma. The Late Cretaceous age (75–85 Ma) is consistent with the zircon U–Pb age of the Shangbao granites (80.1 ± 0.3 Ma) to within uncertainties. Considering also the relatively lower radiogenic initial $^{187}Os/^{188}Os$ ratio of this sample, we suggest that the later stage pyrite ore was probably formed through crystallization from the magmatic hydrothermal fluids. Combined with other geological and associated magmatic data, we propose a skarn-related fluid–ore interaction process to explain the second stage of metallogenesis in the Shangbao pyrite deposit. The Early Permian pyrite ore was deposited in a brine basin with evaporites during the Early Permian. Later magmatic hydrothermal fluids originating from the Shangbao granites, which included mantle components, interacted with the strata and the Early Permian pyrite ore during the Late Cretaceous and precipitated a later stage pyrite ore. During the Late Mesozoic, the roll-back of subducted Paleo-Pacific plate caused lithospheric extension in South China, triggering the upwelling and partial melting of the asthenosphere. The resulting underplating of mantle-derived magmas provided a vast amount of heat and materials for the formation of the granites and polymetallic deposits in South China. Given that the multiple mineralization events were spatially and temporally associated with the Paleozoic–Mesozoic magmatism, the Re–Os isotopic dating of euhedral pyrite grains has been shown to be a viable method for unveiling the evolutionary history of ore-deposits. Skarn development caused by granite and mafic dike emplacement resulting from crust–mantle interaction explains the occurrence of two mineralization episodes at the same locality.

Keywords: Pyrite Re–Os geochronology; Fluid–ore interaction; Skarn; Ore deposit formation; Shangbao; South China

* Corresponding author. State Key Laboratory of Isotope Geochemistry, Guangzhou Institute of Geochemistry, Chinese Academy of Sciences, Guangzhou 510640, China.
E-mail address: wqiang@gig.ac.cn (Q. Wang).
Peer review under responsibility of Guangzhou Institute of Geochemistry.

http://dx.doi.org/10.1016/j.sesci.2017.04.001

1. Introduction

Crustal reworking and crust–mantle interaction are considered to have played important roles in the crustal evolution of South China (Charvet, 2013; Faure et al., 2009; Li et al., 2010a; Shu et al., 2011, 2014; Xu et al., 2007; Wang et al., 2007, 2010; Yu et al., 2016). Paleozoic–Mesozoic magmatic rocks occur widely in South China (Guan et al., 2014; Huang et al., 2013; Li et al., 2010a; Xia et al., 2014; Wang et al., 2013; Yao et al., 2012; Yu et al., 2016; Zhang et al., 2015), and some magmatic rocks have been interpreted to have been related to crustal reworking or remelting or to crust–mantle interaction (Shu et al., 2011; Wang et al., 2013; Xia et al., 2014; Xu et al., 2007; Yu et al., 2016; Zhang et al., 2015). In addition, tungsten, tin, molybdenum, antimony, and bismuth deposits are abundant in South China (Mao et al., 2008, 2013; Sun et al., 2012), with their reserves ranking among the largest in the world (Sun et al., 2012). Most of these deposits are closely associated with contemporary magmatic rocks generated by crustal reworking or crust–mantle interaction (Sun et al., 2012; Mao et al., 2011; Hu et al., 2012; Zaw et al., 2007; Zhou et al., 2006). However, whether crustal reworking or crust–mantle interaction produced the metal mineralization remains unknown. To constrain the mineralization ages, most previous research has concentrated on the veins or host rocks (e.g., magmatic rocks) which were spatially related to the ore deposits. But these methods can only provide indirect rather than direct information on the mineralization ages of the metal deposits. In fact, the mineralization age(s) and, in particular, the origin(s) of the metal cannot be determined by this approach.

The Re–Os isotope system has been widely accepted as a chalcophile system, which could be the "silver bullet" for resolving the mineralization age(s) and the origin(s) of metal deposits (Herr and Merz, 1955). Due to their siderophile and chalcophile nature, Re and Os are incorporated directly into sulfide phases. Therefore, the Re–Os geochronometer can be used for dating the formation age of ore samples directly, and the Re–Os age will represent the true mineralization age of an ore deposit. In addition, Re is more highly concentrated in crustal rocks than Os when compared to the mantle, because Re is more incompatible than Os during mantle melting (Morgan et al., 1981; Walker et al., 1989). With time, crustal rocks tend to develop distinctively higher Re/Os ratios and very radiogenic Os isotopic compositions. Thus, the Re–Os isotopic system is a highly sensitive monitor of the extent of crustal involvement during ore genesis. Compared to the lithophilic Rb–Sr, Sm–Nd, Lu–Hf, and U–Th–Pb isotopic systems, the chalcophile and siderophile nature of Re–Os bestows them with unique advantages in the dating of mineralization age(s) and in determining the origin(s) of metal materials directly (Mathur et al., 1999; Lambert et al., 1998, 1999).

Since the successful application of the method on molybdenite in the 1990s (McCandless et al., 1993; Suzuki et al., 1996; Marcantonio et al., 1994; McCandless, 1994; Huang et al., 1995; Stein et al., 1998, 2001; Du et al., 2001), increasing numbers of scientists have turned their interests to the more ubiquitous metal minerals such as pyrite, arsenopyrite, pyrrhotite, and magnetite. In recent years, Re–Os isotopic analyses applied to these minerals has yielded a significant amount of new geological information (Kerr and Selby, 2012; Mathur et al., 1999, 2000, 2005; Cardon et al., 2008; Liu et al., 2012; Barra et al., 2003; Selby et al., 2009; Zhang et al., 2005; Gannoun et al., 2003; Freydier et al., 1997; Guo et al., 2011; Lü et al., 2011; Feng et al., 2009; Stein et al., 1998; Sun et al., 2008; Han et al., 2007). With the development of the Negative Thermal Ionization Mass Spectrometry (NTIMS) and High-Resolution Inductively Coupled Plasma Mass Spectrometry (HR-ICP-MS) analytical techniques (Volkening et al., 1991; Creaser et al., 1991), determining the low concentrations of Re and Os (at the ppt level) in theses minerals is no longer a limitation. Compared to molybdenite, the high level of common Os in pyrite gives it an important advantage in tracing the origin of metallic minerals.

The Shangbao fluorite crystal deposit, which is associated with the tourmaline-bearing two-mica granite intrusion, is world-renowned for its gigantic pyrite and fluorite crystals. It is also an example of the polymetallic deposits in South China, which include Nb–Ta, W–Sn, and sulfides ore deposits (Lei et al., 2009; Chen et al., 2003). Previous studies have reported the mineral and inclusion characteristics of the Shangbao deposit (Mu et al., 1982; Tu, 1984). Until now, however, no studies have been undertaken on mineralization age and the source of metals has not been established. Consequently, the genetic mechanism responsible for the deposit remains unclear. In this study, we chose two samples with fresh, euhedral, pyrite grains in order to analyze their Re–Os isotope compositions and constrain the mineralization age(s) and origin(s) of the ore. On the basis of these results and other geological and associated geochemical data, we propose that a two-stage process, that includes late fluid–ore interaction, can account for the metallogenesis of the Shangbao pyrite deposit.

2. Geological setting

South China is made up of the Yangtze Block to the northwest and the Cathaysia Block to the southeast (Fig. 1a), and the Hunan Province is located in the central region of South China, at the junction of the Yangtze and Cathaysia Blocks. The Shangbao deposit lies in the southeast part of Hunan Province (Fig. 1a), and is near the Shi-Hang Zone granites (Gilder et al., 1996). The Shi-Hang Zone was first identified by Gilder et al. (1996), and was defined as a belt of granites that are characterized by high concentrations of Sm (>8 ppm) and Nd (>45 ppm), high $\varepsilon Nd(t)$ (>−8), but low t_{DM} (<1.5 Ga) and low initial $^{87}Sr/^{86}Sr$ ratios (<0.710) (Chen and Jahn, 1998; Zhou et al., 2006; Jiang et al., 2008).

Numerous faults and folds occur within the southeast of Hunan Province. The structural features of the Shangbao deposit are dominated by the folding and two faults (Chenzhou-Linwu [CZLW] and Wuhua–Xinshao [WHXS] Faults) (Fig. 1b). Previous studies suggested that the Shangbao

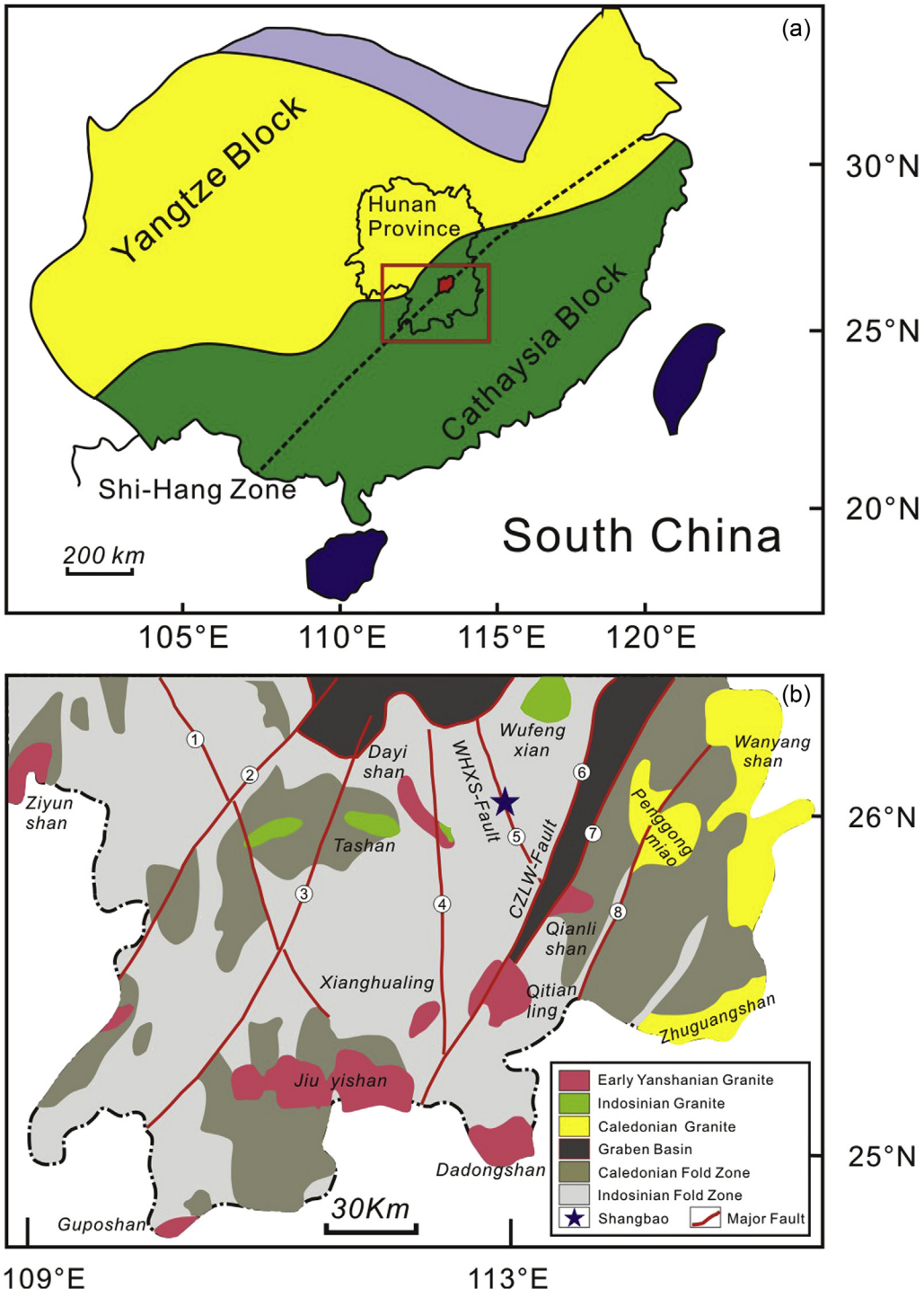

Fig. 1. (a) Simplified geological map of the South China Block. (b) Regional geological map of southern Hunan Province (Modified after Lei et al., 2009).

anticline was formed by Indosinian (or Triassic) tectonic activities (Lei et al., 2009). The core of the anticline is made up of Upper Carboniferous dolomite, while the limbs consist of Lower Permian shale and limestone, with dip angles varying from 35° to 60°. The core and the two limbs are separated by two parallel normal faults, which have a near-NS strike and extend for about 5 km long.

The Shangbao deposit, consisting of nearly pure massive pyrite ore, crops out on the limbs of the anticline. The massive sulfide ores are hosted by the Permian strata, and consist of pyrite grains with a cubic crystal shape (Fig. 3), and rare magnetite grains. Pyrite crystals in the Shangbao deposit are well known as mineral specimens, given that they range in size from several millimeters to about 1 m. The pyrite grains used for this study were about 1 cm in size.

The Shangbao deposit is associated with the Shangbao diabase–granite intrusion. The Shangbao pluton has an outcrop area of less than 2 km^2, occurs near the core of the

anticline, and consists of tourmaline-bearing two-mica granites and diabase dikes (Fig. 2). These dikes have widths ranging from 5 m to 50 m, and their lengths vary from 30 m to 3000 m. The mafic dikes cut through the granite intrusion with steep dip angles ranging from 75° to 90°. The Shangbao granites were emplaced in the Late Cretaceous (zircon U–Pb age: 80.1 ± 0.3 Ma) (Guo, 2013; Guo et al., 2014) and generated skarns in the limestones.

3. Sampling and analytical procedure

3.1. Sampling

Pyrite samples, which contained aggregates of many grains, were collected from the Shangbao sulfide ore deposit, which is located in the Leiyang City, Hunan Province. Individual fresh euhedral pyrite grains were separated from two samples (11SHB01 and 11SHB03) and selected for Re–Os isotope analyses (Fig. 3b). The sample 11SHB03 contains more dolomites in the gap between some pyrite grains than the sample 11SHB01. A total of eleven grains from two samples were picked out and crushed without contacting any steel and tungsten equipment. All mineral powders were prepared by using an agate mortar and pestle set, in order to avoid potential Re contamination. Taking into account the low concentrations of Re and Os in pyrite, coarse grains (diameter > 5 mm) were selected for the Re–Os isotope analyses.

3.2. Analytical method

Re–Os isotopic analyses were carried out in the State Key Laboratory of Isotope Geochemistry, Guangzhou Institute of Geochemistry, Chinese Academy of Sciences (SKLaBIG GIG CAS). About 0.8–0.9 g of powder from each sample was weighed and placed in a Carius tube. Appropriate amounts of the individual Re and Os spike solutions were accurately weighed and carefully added to each sample tube. While the tube was chilled in a bath of a freezing mixture consisting of liquid N_2 and ethanol, 3 ml of concentrated HCl and 9 ml of concentrated HNO_3 were successively added into the tube. The Carius tube was then carefully sealed and heated in an oven at 220 °C for 24 h. After decomposition, the glass tubes were again chilled in a bath containing a freezing mixture of liquid N_2 and ethanol and then opened. After thawing, the contents were poured into 20 ml centrifugation tubes, and after the residual solids were precipitated through centrifugation, the supernatant solutions were transferred into 30 ml PFA vials and subjected to Os solvent extraction by CCl_4 followed by back-extraction into concentrated HBr. The detailed solvent extraction procedure and conditions were described in prior studies (Cohen and Waters, 1996; Pearson and Woodland, 2000). The extracted Os fraction was further purified by microdistillation (Birck et al., 1997) and was then ready for N-TIMS measurement. Osmium was loaded in HBr on 99.999% Pt filaments (H.Cross Company, USA), and $Ba(OH)_2$ emitter solution was loaded on top of the sample to enhance ion emission. Os isotope ratios were measured as the trioxide negative ion (OsO_3^-) on the Thermo Finnigan Triton N-TIMS in negative ion mode, and the Re concentration were measured by Inductively Coupled Plasma Mass Spectrometry (ICP–MS). The details of chemical separations and measurements are described elsewhere (Li et al., 2010b, 2015).

Total procedural blanks (TPB) for this technique were 0.32 ± 0.14 pg with the $^{187}Os/^{188}Os$ ratio of 0.284 ± 0.049 ($n = 2$, 1σ) on average for Os and between 6 and 8 pg for Re. Blank contributions were typically (contribution for sample with lowest concentration in brackets) < 1% (5%) for Re and <3% (37%) for Os, respectively.

The isochronal age was calculated by using the ISOPLOT software (Version 3.7, Ludwig, 1999), and a ^{187}Re decay constant of 1.666×10^{-11} $year^{-1}$ (Smoliar et al., 1996).

4. Analytical results

Eleven grains from two pyrite samples were analyzed and the data are listed in Table 1. The results reveal that the two pyrite samples have different Re–Os isotopic features and yield two distinct isochronal ages (Fig. 4). Both of the samples show a very wide range of $^{187}Re/^{188}Os$ ratios (from 113 to 441,365, and from 18 to 2503, respectively).

Six euhedral pyrite grains from Sample 11SHB01 yield an isochronal age of 279 ± 12 Ma. The Re and Os concentrations vary greatly from 120 to 63,507 ppt and from 2.14 to 185 ppt, respectively. The $^{187}Re/^{188}Os$ and $^{187}Os/^{188}Os$ ratios range from 113 to 441,365 and from 0.66 to 2042, respectively. The initial $^{187}Os/^{188}Os$ ratio is 0.39 ± 0.71 (2σ, $n = 6$). The cause for the uncertainty will be discussed below.

Five euhedral pyrite grains from Sample 11SHB03 give an isochronal age of 75.2 ± 4.3 Ma (Fig. 4). If one pyrite grain with the highest $^{187}Re/^{188}Os$ and $^{187}Os/^{188}Os$ ratios is excluded, the other four pyrite grains give an isochronal age of 85 ± 13 Ma (Fig. 4). Compared to the first stage (~279 Ma) pyrite sample 11SHB01, Sample 11SHB03 has relatively narrow ranges of Re and Os concentrations which vary from 150 to 430 ppt and from 1.0 to 39.9 ppt, respectively. The $^{187}Re/^{188}Os$ and $^{187}Os/^{188}Os$ ratios are also relatively homogeneous except for one point. These isotopic characteristics suggest that most Os was sourced from mantle components derived from either the Shangbao granites or the associated coeval OIB-type mafic dikes (Guo, 2013). The initial $^{187}Os/^{188}Os$ ratio of the sample is 0.141 ± 0.030 (2σ, $n = 5$), and the much lower uncertainty suggests that the result is suitable for assessing mineralization age and metallogenic processes at the deposit.

5. Discussion

5.1. Episodes of mineralization

The pyrite grains from two samples of the Shangbao deposit yield two distinct isochronal ages (Fig. 4). The first stage pyrites were formed at the Early Permian (ca. 279 Ma), which is consistent with that of the strata in which the pyrite deposit was hosted. The late stage pyrites were generated in the Late

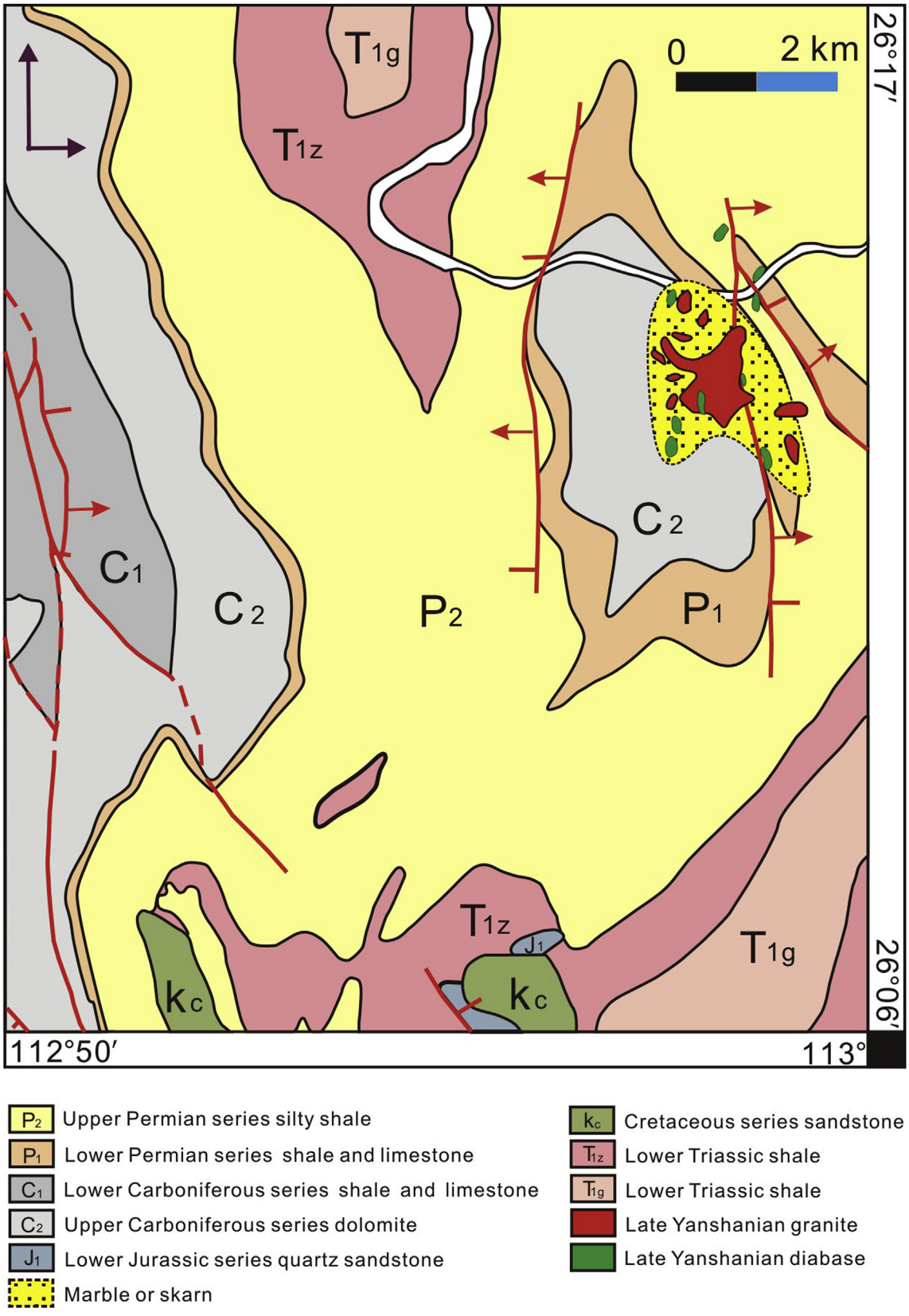

Fig. 2. Regional geological map of the Shangbao area.

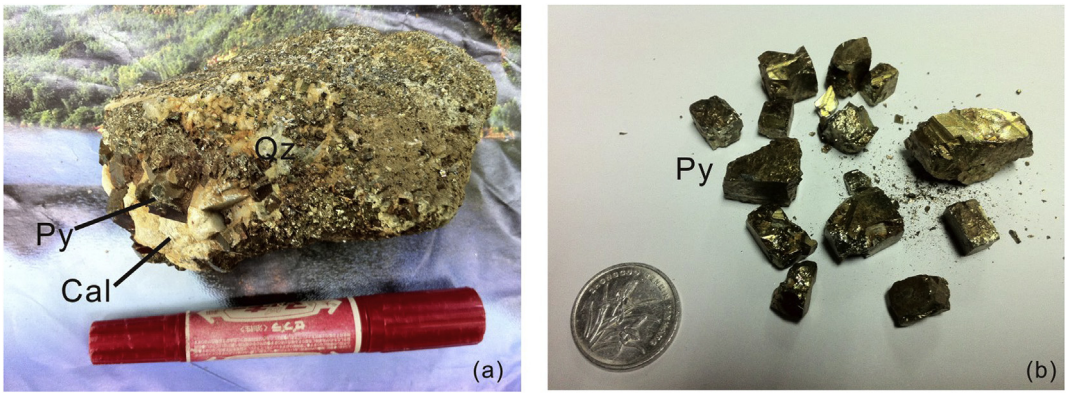

Fig. 3. Photographs of pyrite samples. (a) Massive sulfide ore, Pyrite (Py) + Calcite (Cal) + Quartz (Qz). (b) Single euhedral pyrite grains separated from (a).

Table 1
Re–Os isotope data for the pyrite grains from the Shangbao deposit, southeastern Hunan province, South China.

Sample number	Re_{Total} (ppt)	2σ	Os_{Total} (ppt)	2σ	$^{187}Os/^{188}Os$ Ratio	2σ	$^{187}Re/^{188}Os$ Ratio	2σ	Os_{Common} (ppt)	2σ	Re/Os ratio	TMa
11SHB03-1	216	14	4.49	0.02	0.4716	0.0045	242	16	4.302	0.015	50.28	85
11SHB03-2	432	13	39.9	1.5	0.1939	0.0022	52.6	2.5	39.6	1.6	10.90	74
11SHB03-3	179	8	38.2	1.7	0.1548	0.0023	18.8	1.3	38.2	1.7	3.90	83
11SHB03-4	213	6	8.56	0.37	0.2994	0.0072	123	6	8.39	0.37	25.42	83
11SHB03-5	354	10	0.96	0.01	3.260	0.050	2503	72	0.6792	0.0085	521.19	75
11SHB01-1	340	21	15.49	0.61	0.658	0.021	113	8	14.50	0.62	23.45	282
11SHB01-2	9517	141	45.48	0.25	12.85	0.15	2681	42	16.95	0.31	561.48	285
11SHB01-3	121	3	2.14	0.02	1.689	0.037	328	9	1.775	0.019	68.09	286
11SHB01-4	194	8	2.86	0.01	1.908	0.021	402	16	2.3206	0.0091	83.65	266
11SHB01-5	63,507	874	185	3	2042	54	441,365	9441	0.6825	4	93,046	278
11SHB01-6	3138	59	16.92	0.08	11.84	0.11	2258	43.	6.64	0.090	472.81	312

Note: 1. $Os_{Total} = Os_{Common} + {}^{187}Os_{Total} - {}^{187}Os_{Common}$, where $^{187}Os_{Common} = Os_{Common} \times 0.01926$. 2. Os in Re/Os is common Os, Common Os and common ^{187}Os are calculated according to the Nier value. 3. ^{187}Re decay constant = 1.666×10^{-11} y^{-1} (Smoliar et al., 1996); all data here are blank-corrected.

Cretaceous (75–85 Ma), which is consistent with the zircon U–Pb age (80.12 ± 0.34 Ma) of the associated Shangbao granites (Guo, 2013; Guo et al., 2014). These age data suggest that there are two episodes of mineralization in the Shangbao area.

5.2. Source of metals

The pyrite grains formed during the early stage exhibit different Re and Os isotopic compositions from those formed in the late stage. The early pyrite grains exhibit more variable contents of Re and Os and a wider range of $^{187}Re/^{188}Os$ and $^{187}Os/^{188}Os$ ratios than those of the late pyrite grains. The variable compositions of pyrite grains from the same sample show vast differences in Re and Os concentrations, which were caused by "nugget effects". Such effects may be due to the heterogeneous distribution of the various sulfide populations in whole rock (Alard et al., 2002), because Re and Os might be concentrated in micro-phases that are not equally distributed. Alternatively, the Re and Os may have been derived from a rapidly evolving fluid, where the concentrations are continually changing as different minerals precipitate (Freydier et al., 1997). These effects are advantageous for determining the Re–Os geochronology of sulfides.

The initial $^{187}Os/^{188}Os$ ratio of Sample 11SHB01 is 0.39 ± 0.71 (2σ, $n = 6$), which is much more radiogenic than chondrite ($^{187}Os/^{188}Os = 0.125$) at 279 Ma (Meisel et al., 1996). The radiogenic initial $^{187}Os/^{188}Os$ ratio may indicate a significant contribution from felsic crust, particularly since crustal melts have low Os concentrations compared to mantle melts (Freydier et al., 1997). For example, the Re/Os vs. common Os diagram (Fig. 5) displays a wide field for Sample 11SHB01 (one point was excluded for its high proportion of radiogenic ^{187}Os and extremely low common Os concentration like molybdenite) that is not entirely consistent with the mantle melts array. The relatively large uncertainty comes from the following sources:

(1) The low concentrations of common Os and abundant radiogenic ^{187}Os components may have resulted in an underestimate of the analytical error. Sample 11SHB01 has low common Os concentrations and high proportions of radiogenic ^{187}Os components (accounting for 8–99.6% of total Os) compared to Sample 11SHB03 (usually lower than 10%). These two factors allow analytical blank errors to make much larger contributions to uncertainties in the $(^{187}Os/^{188}Os)_i$ ratios and Sample 11SHB01 does display a wide range of $(^{187}Os/^{188}Os)_i$ ratios (0.0332–1.3185),

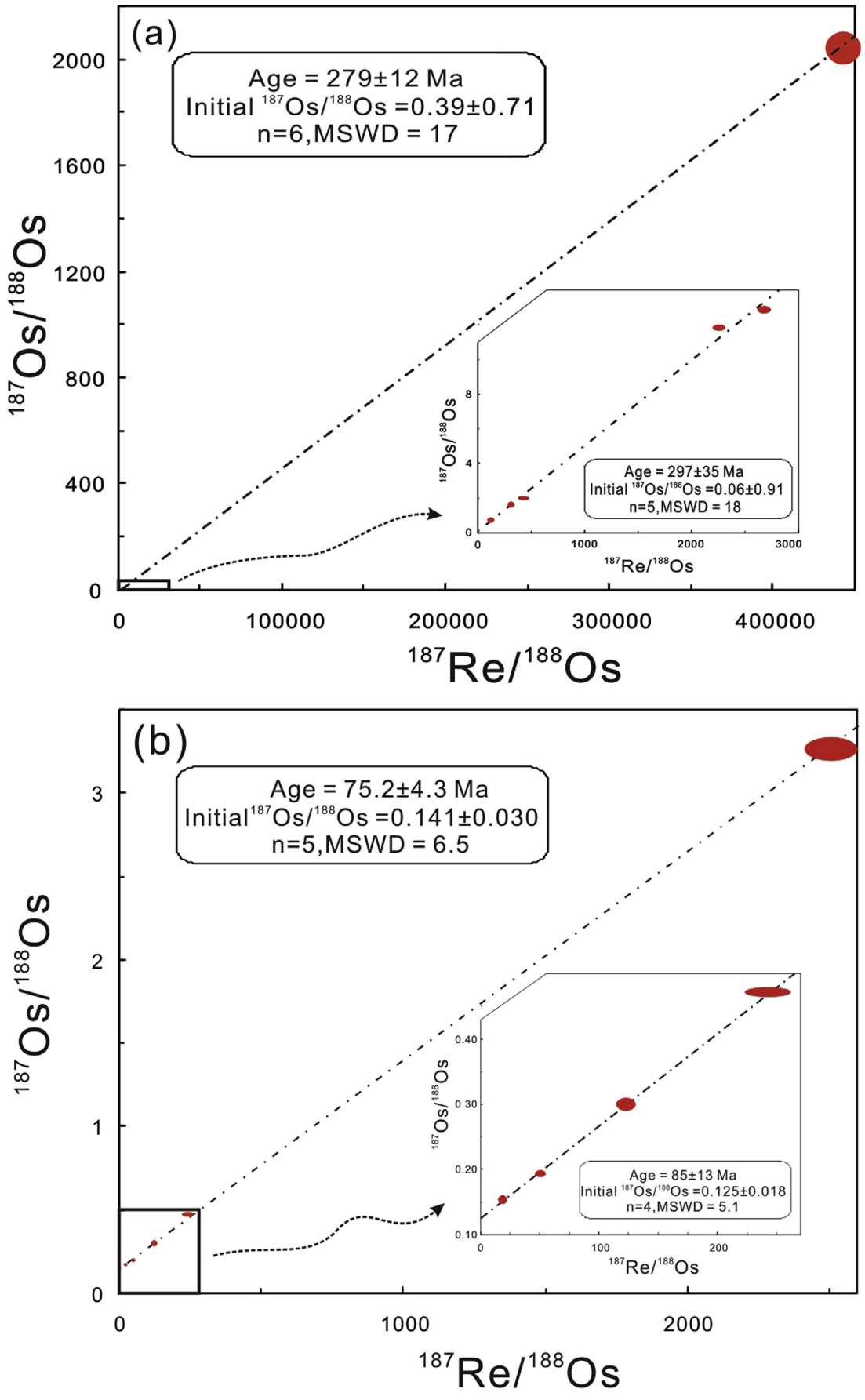

Fig. 4. Re–Os isochronal ages for pyrites from the Shangbao deposit. (a) The isochronal age of Sample 11SHB01. (b) The isochronal age of Sample 11SHB03.

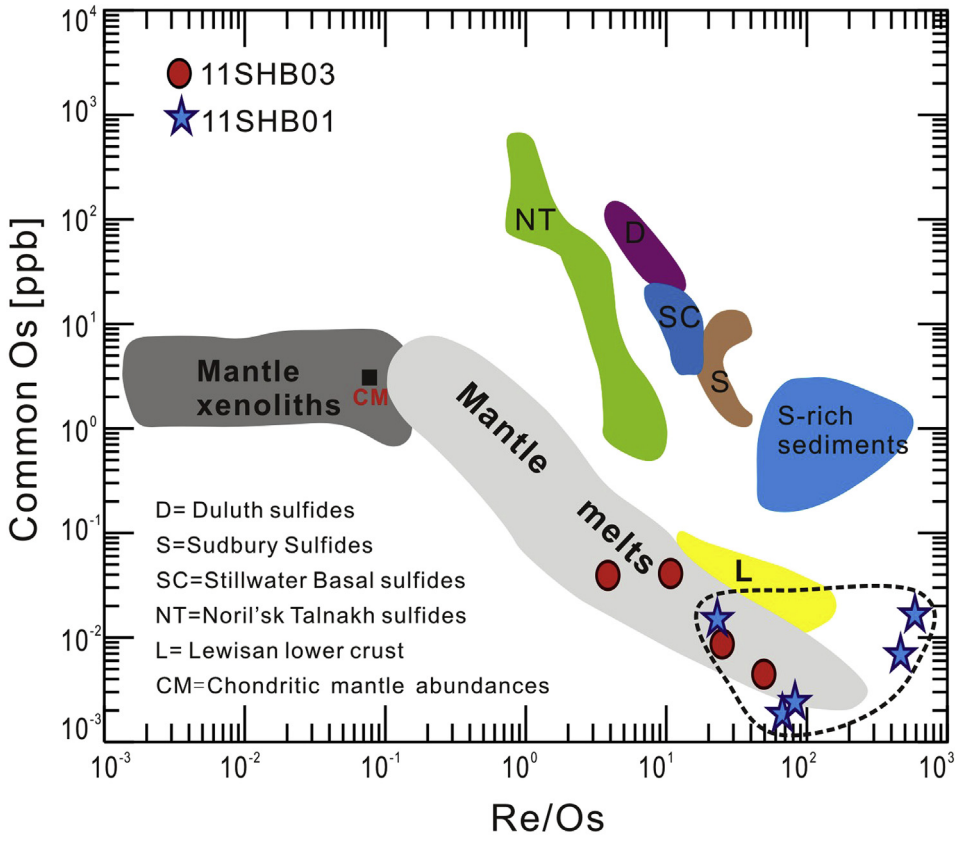

Fig. 5. Re/Os vs. common Os concentrations (Os concentration at the time of ore formation) (modified after Lambert et al., 1998). Duluth Complex (Ripley et al., 1999), Sudbury (Walker et al., 1991), and Noril'sk–Talnakh (Walker et al., 1994); Archean lithospheric mantle xenoliths from the Kaapvaal and Siberian Cratons (Walker et al., 1989); mantle melts, which include komatiites (Walker et al., 1988; Foster et al., 1996) and basalts (Martin, 1991; Hauri and Hart, 1993; Snow and Reisberg, 1995); Lewisian lower crustal gneisses (Frick et al., 1996); metalliferous S-rich sediments (Ravizza and Turekian, 1992); and chondritic mantle abundances (Walker and Morgan, 1989).

calculated by formula $(^{187}Os/^{188}Os)_i = (^{187}Os/^{188}Os)_m - (^{187}Re/^{188}Os) * (e^{\lambda t} - 1)$.

(2) The Re–Os system may have been disturbed slightly by later magmatic event, or some other process that caused a redistribution of Re and radiogenic Os. There is, however, no microscopic evidence of supergene alteration because all of the chosen euhedral pyrite grains had fresh unoxidized surfaces and had no inclusions. According to Brenan et al. (2000), the pyrite grains at millimeter-size can undergo core disturbances by a diffusive exchange with an external Os reservoir, and the process could occur for at least 10 Ma at 500 °C. The radii of all pyrite grains in this research are about 5 mm, however, which are large enough to resist supergene diffusive exchanges. Stein et al. (1998) and Selby and Creaser (2001) suggested that the Re–Os systematics are unaffected by post-ore processes. Selby and Creaser (2001) also concluded that the Re–Os system was undisturbed by low to moderately saline (1–15 wt% NaCl equiv.) hydrothermal fluids. Selby et al. (2009) worked on the Ruby Creek deposit, and their results show that the Re–Os systematics of pyrite, chalcopyrite, and bornite were unaffected by greenschist facies metamorphism. All these data indicate that the Re–Os isotope system is very resistant to later disturbances. The Re and Os concentrations of the late pyrite grains are much lower than the early pyrite grains in the Shangbao ore deposit, and it seems that Re–Os isotope system of the sampled early pyrite grains did not undergo later metamorphic disturbances.

(3) A complex precipitation process in a syn-sedimentary deposit may contribute to large uncertainties. Table 1 displays the heterogeneous Re–Os isotopic features of Sample 11SHB01, although the Re–Os age is consistent with that of the strata that host the pyrite deposit. It is reasonable to infer that the early pyrite grains are a type of syn-sedimentary deposit (Feng et al., 2009). In addition, no geological data suggest that a magmatic event was responsible for the formation of the early pyrite grains. Regional geological data also show that between the Neoproterozoic to the Early Triassic, the entire area was a shallow sea–coastal region where precipitated sedimentary limestone and (or) coal bearing formations were continually and steadily formed (Fig. 2). Clearly, a formation model for the syn-sedimentary deposit may be complicated by the numerous potential Os sources for the deposit.

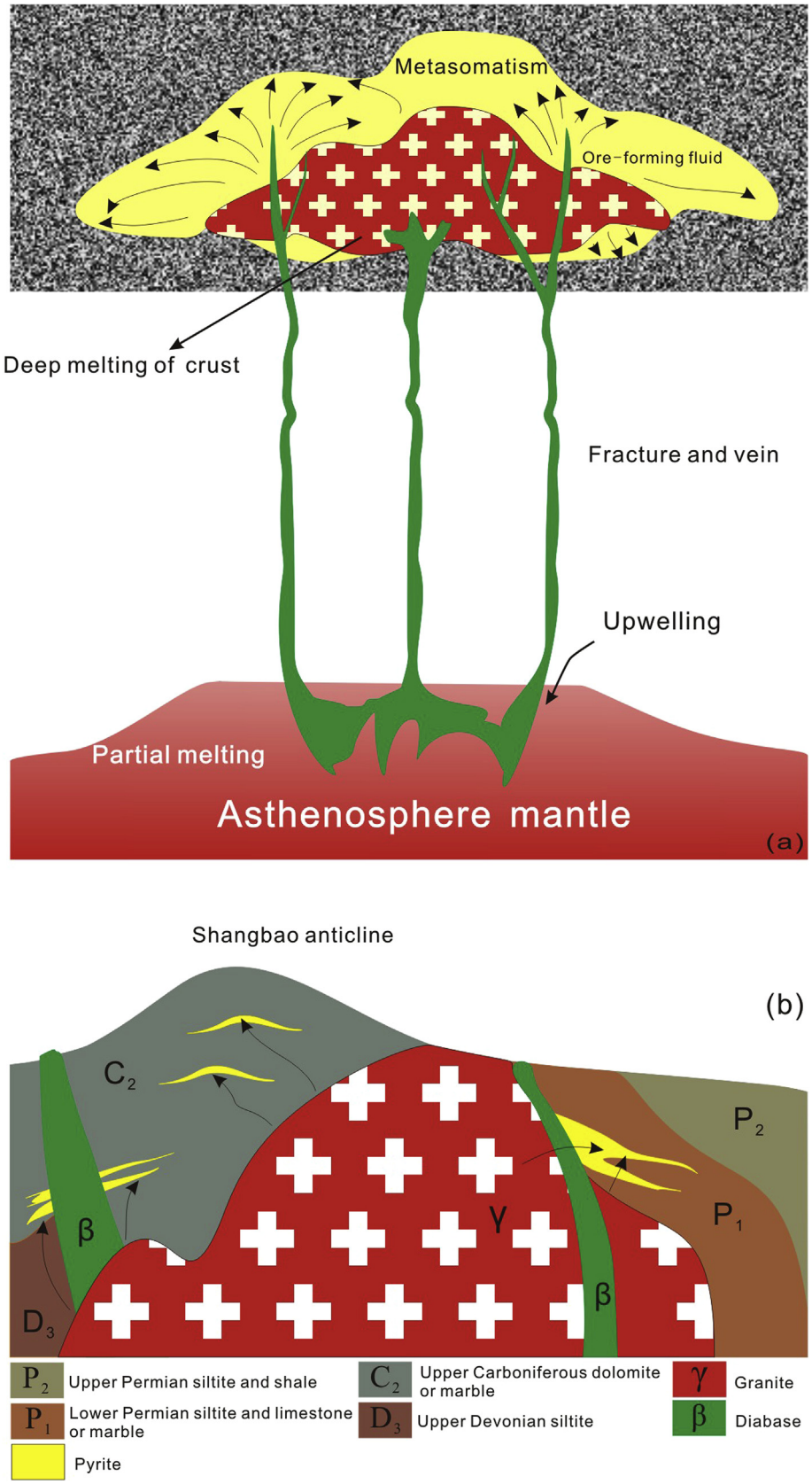

Fig. 6. Metallogenic model of the Shangbao pyrite deposit (modified after Kemp et al., 2007). (a) The Early Permian pyrite ore was formed by syn-sedimentary precipitation. (b) Emplacement of granite and mafic dikes in the core of the Shangbao anticline provided an ideal location for the precipitation of late stage pyrite grains in a skarn environment.

It is difficult to determine how metals were initially introduced to the deposit because the strata were heavily reworked by late stage skarn formation caused by the granite. There are two main types of models for the syn-sedimentary deposit formation: (1) the theory of magmatic ore genesis by submarine exhalation on the seafloor is now widely accepted (Guo et al., 2011; Feng et al., 2009; Gu et al., 2012; Han and Hutchinson, 1989; Gu and Xu, 1986; Pasava et al., 1996; Lott et al., 1999). Magmatic hydrothermal fluids rise through fractures and veins and thus take metal materials to the surface. (2) Metals are leached from the country rocks or an igneous Os reservoir by meteoric water or seawater or that has been heated and modified during convection to become a hydrothermal fluid, or a mixture of these types of fluids (Mathur et al., 1999, 2000; Munha and Kerrich, 1980; Kesler et al., 2002; Kirk et al., 2002; Freydier et al., 1997). Re and Os can be scavenged efficiently by anoxic sea-bottom sediments (Ravizza et al., 1991), and under such anoxic environments, which generally have a low sedimentation rate, metal element concentrations in some black shales can be enriched compared to seawater by factors of 10^5 to 10^6 (Holland, 1979). Sulfides precipitated by this process usually have the same initial $^{187}Os/^{188}Os$ ratios as the seawater, while the present day average seawater has $^{187}Os/^{188}Os = 1.04 \pm 0.04$ (Sharma et al., 1997).

Because no magmatic sources as required for Model 1 are known, and the initial $^{187}Os/^{188}Os$ ratios are much less radiogenic than seawater, we propose that Model 2 is more plausible for the formation of the Early Permian pyrite grains.

Relatively narrow ranges of Re and Os isotopic characteristics indicate an isotopically homogeneous source (Mathur et al., 2000, 2005; Freydier et al., 1997). Combined with an age consistent with the Shangbao granites, the late stage pyrite grains were probably formed by magmatic hydrothermal fluids. The $(^{187}Os/^{188}Os)_i$ ratios have a limited range from 0.128 to 0.168, with an average of 0.141 ± 0.030 (Fig. 4). This value is basically close to the chondrite at 75 Ma ($^{187}Os/^{188}Os = 0.1296$) (Meisel et al., 1996), which indicates that mantle materials played a dominant role in the formation of the late stage pyrite grains. The Re/Os vs. common Os diagram (Fig. 5) also displays a trend that is approximates the array for mantle melts. In addition, the Shangbao pyrite ore deposit is closely associated with the contemporary Shangbao granites and coeval OIB-type mafic dikes (Guo, 2013) that represent a plausible source for mantle components in the metallic deposit.

5.3. Geological implications

Fluid–ore interaction can explain why two mineralization episodes are identified in close association. Combining the new data with regional geological observations, we infer the Early Permian pyrite grains were formed by syn-sedimentary precipitation (Fig. 6b). Since the Early Paleozoic, the whole region of South China was a passive continental margin which was covered by seawater (Fig. 3) (Li and Li, 2007; Li et al., 2012). Meteoric fluids from continental sources and hydrothermal fluids that leached metals from mafic intrusions or seafloor basalts of early period would have precipitated synchronously within sedimentary strata in this setting. The initial $^{187}Os/^{188}Os$ ratio reveals a mantle-dominated metal source but with a significant contribution from crustal sources during the ore formation process, which is consistent with our results.

The tectonic setting of the SCB gradually changed from compressional to extensional during the Mesozoic. This phenomenon was related to either the subduction of the Paleo-Pacific oceanic plate beneath the Chinese continent (Xu and Xie, 2005; Zhou et al., 2006; Jiang et al., 2009), or an intracontinental rifting (Fan et al., 2003; Li et al., 2003, 2004; Wang et al., 2003). This lithospheric extension continued from the Jurassic to the Cretaceous, and increased mantle–crust interaction (i.e., emplacement of mantle magmas and higher heat flow) is well established for this interval (Jiang et al., 2011; Liu et al., 2012; Li and Li, 2007; Xu et al., 2007; Wang et al., 2003, 2008; Li et al., 2012). The local tectonic setting of southeastern Hunan Province was consistent with the larger-scale tectonic environment of South China (Fig. 2). An association of graben basins and deep fractures implies extension of the lithosphere. The CZLW-fault was reactivated in the Triassic, and evolved into a strike-slip fault in the Jurassic–Cretaceous, and finally developed into a graben basin (Wang et al., 2003, 2008). A steeper subduction dip angle and the rollback of the subducted Pacific plate in the Late Cretaceous are considered to have been responsible for the formation of vast volumes of coeval granites (Li and Li, 2007; Zhou et al., 2006; Jiang et al., 2009; Li et al., 2012). The OIB-like geochemical features of the Late Cretaceous Shangbao mafic dikes intruding the granite pluton suggest that they were derived from asthenospheric mantle where upwelling was triggered by the crustal extension (Guo, 2013). The rising basaltic magmas provided the heat source for crustal melting. Due to the heat of magmas and metasomatism induced by metal-carrying magmatic hydrothermal fluids, the early strata were strongly recrystallized, as evidenced by skarn development around the pluton. Pyritization is associated with the skarn-forming event. The in situ magmatic hydrothermally precipitated pyrite grains caused the phenomenon of two stage pyrite symbiosis in the same area. The core of the Shangbao anticline provided an ideal space for the precipitation of late stage pyrite grains. The crystal deposit was formed under a fluoride fluid enrichment conditions (Fig. 6a).

The Re–Os isotope data of the Shangbao pyrite deposit suggest that mantle materials have made significant contributions to the formation of Paleozoic–Mesozoic polymetallic deposits in South China. Multiple episodes of mineralization are associated with widespread Mesozoic magmatic events and, in at least some cases, they have overprinted earlier syn-sedimentary mineralization.

6. Conclusions

Rhenium and osmium elemental and isotopic data have been obtained for the Shangbao pyrite deposit in the southeastern Hunan Province. The two pyrite samples collected

from the same locality yield distinct ages. One sample yields an isochronal age of 279 ± 12 Ma and an initial $^{187}Os/^{188}Os$ ratio of 0.39 ± 0.71, the other yields an isochronal age of 75.2 ± 4.3 Ma or 85 ± 13 Ma, with an initial $^{187}Os/^{188}Os$ ratio of 0.141 ± 0.030.

The first stage pyrite grains were formed synchronously with sedimentary strata from a mantle-dominated metal source, but also contain a component leached by meteoric water or hydrothermal fluids that contained a significant crustal contribution. The late stage pyrite grains were formed by crystallization from the magmatic hydrothermal fluids during skarn formation in local limestones. The ore-forming metal was almost entirely derived from the mantle with only slight contamination from crustal sources. This result implies a significant contribution of mantle materials to Mesozoic polymetallic deposit formation in South China.

Fluid-reprocessing during skarn formation increased the mantle contribution to a younger ore-forming episode compared to the syn-sedimentary event. Crust−mantle interaction in the form of granite and dike emplacement at shallow crustal levels ultimately explains the existence of two mineralization episodes at a single locality. Rollback of the subducted Pacific Plate in the Late Cretaceous caused a widespread extensional regime in the South China Block. Enormous volumes of hot mantle magmas ascended into the shallow crust, which provided large amounts of heat and materials for the formation of both granites and polymetallic mineralization in South China.

Acknowledgments

We would like to thank Editor-in-Chief Professor Wei-Dong Sun, and two anonymous reviewers for their very constructive and helpful reviews. We appreciate the assistance of Professor Ji-Feng Xu and Drs. Gui-Qing Wang and Pei-Pei Zhao for Re−Os isotope analyses. Financial support for this research was provided by the DREAM Program of China (No. 2016YFC0600407), the Key Program of the Chinese Academy of Sciences (QYZDJ-SSW-DQC026), the Strategic Priority Research Program (B) of the Chinese Academy of Sciences (Grant No. XDB03010600), the National Natural Science Foundation of China (Nos. 41630208 and 41421062), the Talent Project of Guangdong Province (2014TX01Z079), and GIGCAS 135 project 135TP201601. This is contribution IS-2585 from GIGCAS.

References

Alard, O., Griffin, W.L., Pearson, N.J., Lorand, J.P., O'Reilly, S.Y., 2002. New insights into the Re−Os systematics of sub-continental lithospheric mantle from in situ analysis of sulphides. Earth Planet. Sci. Lett. 203 (2), 651−663.

Barra, F., Ruiz, J., Mathur, R., Titley, S., 2003. A Re−Os study of sulfide minerals from the Bagdad porphyry Cu−Mo deposit, northern Arizona, USA. Miner. Deposita 38 (5), 585−596.

Birck, J.L., Roy Barman, M., Capmas, F., 1997. Re−Os isotopic measurements at the femtomole level in natural samples. Geostand. Newsl. 20, 19−27.

Brenan, J.M., Cherniak, D.J., Rose, L.A., 2000. Diffusion of osmium in pyrrhotite and pyrite implications for closure of the Re−Os isotopic system. Earth Planet. Sci. Lett. 180 (3−4), 399−413.

Cardon, O., Reisberg, L., Andre-Mayer, Anne-Sylvie, Leroy, J., Milu, V., Zimmermann, C., 2008. Re−Os systematics of pyrite from the Bolcana porphyry copper deposit, Apuseni Mountains, Romania. Econ. Geol. 103 (8), 1695−1702.

Charvet, J., 2013. The Neoproterozoic−Early Paleozoic tectonic evolution of the South China block: an overview. J. Asian Earth Sci. 74, 198−209.

Chen, J.F., Jahn, B.M., 1998. Crustal evolution of southeastern China: Nd and Sr isotopic evidence. Tectonophysics 284 (1−2), 101−133.

Chen, X.L., Jin, Y.H., Xie, C.G., 2003. Occurrence of niobium and tantalum in the Nb−Ta deposit in weathered granite crust at Shangbao, Leiyang, Hunan Province. Acta Mineral. Sin. 23 (4), 323−326 (in Chinese with English abstract).

Cohen, A.S., Waters, G.G., 1996. Separation of osmium from geological materials by solvent extraction for analysis by thermal ionization mass spectrometry. Anal. Chim. Acta 332, 269−275.

Creaser, R.A., Papanastassiou, D.A., Wasserburg, G.J., 1991. Negative thermal ion mass spectrometry of osmium, rhenium, and iridium. Geochim. Cosmochim. Acta 55 (1), 397−401.

Du, A.D., Zhao, D.M., Wang, S.X., Sun, D.Z., Liu, D.Y., 2001. Precise Re−Os dating for molybdenite by ID-NTIMS with Carius tube sample preparation. Rock Miner. Anal. 20 (4), 247−252 (in Chinese with English abstract).

Fan, W.M., Wang, Y.J., Guo, F., Peng, T.P., 2003. Mesozoic mafic magmatism in Hunan-Jiangxi provinces and the lithospheric extension. Earth Sci. Front. 10 (3), 159−169 (in Chinese with English abstract).

Faure, M., Shu, L.S., Wang, B., Charvet, J., Choulet, F., Monié, P., 2009. Intracontinenal subduction: a possible mechanism for the Early Paleozoic Orogen of SE China. Terra Nova 21 (5), 360−368.

Feng, C.Y., Qu, W.J., Zhang, D.Q., Dang, X.Y., Du, A.D., Li, D.X., She, H.Q., 2009. Re−Os dating of pyrite from the Tuolugou stratabound Co(Au) deposit, eastern Kunlun Orogenic Belt, northwestern China. Ore Geol. Rev. 36 (1−3), 213−220.

Freydier, C., Ruiz, J., Chesley, J., McCandless, T., Munizaga, F., 1997. Re−Os isotope systematics of sulfides from felsic igneous rocks: application to base metal porphyry mineralization in Chile. Geology 25 (9), 775−778.

Frick, L.R., Lambert, D.D., Cartwright, I., 1996. Re−Os dating of metamorphism in the Lewisian complex, NW Scotland: Goldschmidt Symposium Heidelberg. J. Conf. Abstr. 11, 185.

Foster, J.G., Lambert, D.D., Frick, L.R., Maas, R., 1996. Re−Os isotopic evidence for genesis of Archaean nickel ores from uncontaminated komatiites. Nature 382, 703−706.

Gannoun, A., Tessalina, S., Bourdon, B., Orgeval, J.J., Birck, J.L., Allègre, C.J., et al., 2003. Re−Os isotopic constraints on the genesis and evolution of the Dergamish and Ivanovka Cu (Co, Au) massive sulphide deposits, south Urals, Russia. Chem. Geol. 196 (1−4), 193−207.

Gilder, S.A., Gill, J., Coe, R.S., Zhao, X.X., Liu, Z.W., Wang, G.X., Yuan, K.R., Liu, W.L., Kuang, G.D., Wu, H.R., 1996. Isotopic and paleomagnetic constraints on the Mesozoic tectonic evolution of South China. J. Geophys. Res. 101 (7), 137−152.

Gu, L.X., Xu, K.Q., 1986. On the South China type massive sulfide ore deposits formed in marine fault depression troughs on the continental crust. Miner. Deposits 5 (2), 1−13 (in Chinese with English abstract).

Gu, X.X., Zhang, Y.M., Schulz, O., Vavtar, F., Liu, J.M., Zheng, M.H., Zheng, L., 2012. The Woxi W−Sb−Au deposit in Hunan, South China: an example of Late Proterozoic sedimentary exhalative (SEDEX) mineralization. J. Asian Earth Sci. 57, 54−75.

Guan, Y.L., Yuan, C., Sun, M., Wilde, S., Long, X.P., Huang, X.L., Wang, Q., 2014. I-type granitoids in the eastern Yangtze Block: implications for the Early Paleozoic intracontinental orogeny in South China. Lithos 206−207, 34−51.

Guo, H.F., Xia, X.P., Wei, G.J., Wang, Q., Zhao, Z.H., Huang, X.L., Yuan, C., Li, W.X., 2014. LA-MC-ICPMS in-situ boron isotopic analyses of tourmalines from the Shangbao granites (southern Hunan Province) and its geological significance. Geochemica 43 (1), 11−19 (in Chinese with English abstract).

Guo, H.F., 2013. Petrogenesis of Late Cretaceous Tourmaline-bearing Two-mica Granites and Associated Mafic Dikes in the Shangbao Area, Southern Hunan Province: Implications for Dynamics and Metallogenesis (Dissertation). University of Chinese Academy of Sciences (in Chinese with English abstract).

Guo, W.M., Lu, J.J., Jiang, S.Y., Zhang, R.Q., Qi, L., 2011. Re−Os isotope dating of pyrite from the footwall mineralization zone of the Xinqiao deposit, Tongling, Anhui Province: geochronological evidence for submarine exhalative sedimentation. Chin. Sci. Bull. 56 (35), 3860−3865 (in Chinese with English abstract).

Han, C.M., Xiao, W.J., Zhao, G.C., Qu, W.J., Du, A.D., 2007. Re−Os dating of the Kalatongke Cu−Ni deposit, Altay Shan, NW China, and resulting geodynamic implications. Ore Geol. Rev. 32 (1−2), 452−468.

Han, F., Hutchinson, R.W., 1989. Evidence for the exhalative hydrothermal sedimentary origin of the Dachang Sn-polymetal deposit − trace element and rare earth element geochemistry of the host rocks. Miner. Deposits 8 (3), 33−44 (in Chinese with English abstract).

Hauri, E., Hart, S., 1993. Re−Os isotope systematic of HIMU and EMII oceanic Island basalts from the South Pacific ocean. Earth Planet. Sci. Lett. 114 (2−3), 353−371.

Herr, W., Merz, E., 1955. Eine neue Methode zur Alterbestimmung von Rhenium-haltigen Mineralien mittels Neutronenaktivienmg. Zeitsch. Naturforsch. 10 (1), 613−615.

Holland, H.D., 1979. Metals in black shales—a reassessment. Econ. Geol. 74 (7), 1676−1680.

Hu, R.Z., Wei, W.F., Bi, X.W., Peng, J.T., Qi, Y.Q., Wu, L.Y., Chen, Y.W., 2012. Molybdenite Re−Os and muscovite $^{40}Ar/^{39}Ar$ dating of the Xihuashan tungsten deposit, central Nanling district, South China. Lithos 150, 111−118.

Huang, D.H., Wu, C.Y., Du, A., He, H.L., 1995. Re−Os isotope ages of molybdenum deposits in East Qinling and their significance. Chin. J. Geochem. 14 (4), 313−322.

Huang, X.L., Yu, Y., Li, J., Tong, L.X., Chen, L.L., 2013. Geochronology and petrogenesis of the early Paleozoic I-type granite in the Taishan area, South China: middle-lower crustal melting during orogenic collapse. Lithos 177, 268−284.

Jiang, S.Y., Zhao, K.D., Jiang, Y.H., Dai, B.Z., 2008. Characteristics and genesis of Mesozoic A-type granites and associated mineral deposits in the southern Hunan and northern Guangxi provinces along the Shi-Hang belt. South China 14 (4), 496−509 (in Chinese with English abstract).

Jiang, Y.H., Jiang, S.Y., Dai, B.Z., Liao, S.Y., Zhao, K.D., Ling, H.F., 2009. Middle to late Jurassic felsic and mafic magmatism in southern Hunan province, southeast China: implications for a continental arc to rifting. Lithos 107 (3−4), 185−204.

Jiang, Y.H., Zhao, P., Zhou, Q., Liao, S.Y., Jin, G.D., 2011. Petrogenesis and tectonic implications of Early Cretaceous S- and A-type granites in the northwest of the Gan-Hang rift, SE China. Lithos 121 (1−4), 55−73.

Kemp, A.I., Hawkesworth, C.J., Foster, G.L., Paterson, B.A., Woodhead, J.D., Hergt, J.M., Gray, C.M., Whitehouse, M.J., 2007. Magmatic and crustal differentiation history of granitic rocks from Hf−O isotopes in zircon. Science 315 (5814), 980−983.

Kerr, A., Selby, D., 2012. The timing of epigenetic gold mineralization on the Baie Verte Peninsula, Newfoundland, Canada: new evidence from Re−Os pyrite geochronology. Miner. Deposita 47 (3), 325−337.

Kesler, S.E., Chryssoulis, S.L., Simon, G., 2002. Gold in porphyry copper deposits its abundance and fate. Ore Geol. Rev. 21 (1−2), 103−124.

Kirk, J., Ruiz, J., Chesley, J., Walshe, J., England, G., 2002. A major Archean, gold and crust-forming event in the Kaapvaal craton, South Africa. Science 297 (5588), 1856−1858.

Lambert, D.D., Foster, G.L., Frick, L.R., Li, C., Naldrett, A.J., 1999. Re−Os isotopic systematics of the Voisey's Bay Ni−Cu−Co magmatic ore system, Labrador, Canada. Lithos 47 (1−2), 69−88.

Lambert, D.D., Foster, J.G., Frick, L.R., Ripley, E.M., Zientek, M.L., 1998. Geodynamics of magmatic Cu−Ni−PGE sulfide deposits: new insights from the Re−Os isotope system. Econ. Geol. Bull. Soc. 93 (2), 121−136.

Lei, Z.H., Qiao, Y.S., Xu, Y.M., 2009. W−Sn mineralization characteristics and exploration potential of the Shangbao mineral district, Hunan province. Geol. Explor. 45 (2), 44−52 (in Chinese with English abstract).

Li, J., Zhao, P.P., Liu, J.G., Wang, X.C., Yang, Y., Wang, G.Q., Xu, J.F., 2015. Reassessment of hydrofluoric acid desilicification in the Carius tube digestion technique for Re−Os isotopic determination in geological samples. Geostand. Geoanal. Res. 39 (1), 17−30.

Li, J., Zhong, L.F., Tu, X.L., Liang, X.R., Xu, J.F., 2010b. Determination of rhenium content in molybdenite by ICP−MS after separation of the major matrix by solvent extraction with N-benzoyl-N-phenylhydroxalamine. Talanta 81, 954−958.

Li, X.H., Chen, Z.G., Liu, D.Y., Li, W.X., 2003. Jurassic gabbro-granite−syenite suites from southern Jiangxi Province (SE China): age, origin and tectonic significance. Int. Geol. Rev. 45, 898−921.

Li, X.H., Chung, S.L., Zhou, H.W., Lo, C.H., Liu, Y., Chen, C.H., 2004. Jurassic intraplate magmatism in southern Hunan-eastern Guangxi: $^{40}Ar/^{39}Ar$ dating, geochemistry, Sr−Nd isotopes and implications for tectonic evolution of SE China. In: Malpas, J., Fletcher, C.J., Aitchison, J.C., Ali, J. (Eds.), Aspects of the Tectonic Evolution of China, vol. 226. Geol Soc Lond Spec Pub, pp. 193−216.

Li, Z.X., Li, X.H., 2007. Formation of the 1300-km-wide intracontinental orogen and post-orogenic magmatic province in Mesozoic South China: a flat-slab subduction model. Geology 35 (2), 179−182.

Li, Z.X., Li, X.H., Chung, S.L., Lo, C.H., Xu, X.S., Li, W.X., 2012. Magmatic switch-on and switch-off along the South China continental margin since the Permian: transition from an Andean-type to a Western Pacific-type plate boundary. Tectonophysics 532−535, 271−290.

Li, Z.X., Li, X.H., Wartho, J.A., Clark, C., Li, W.X., Zhang, C.L., Bao, C., 2010a. Magmatic and metamorphic events during the Early Paleozoic Wuyi-Yunkai Orogeny, southeastern South China: new age constraints and pressure−temperature conditions. Geol. Soc. Am. Bull. 122 (5−6), 772−793.

Liu, C.Z., Liu, Z.C., Wu, F.Y., Chu, Z.Y., 2012. Mesozoic accretion of juvenile sub-continental lithospheric mantle beneath South China and its implications: geochemical and Re−Os isotopic results from Ningyuan mantle xenoliths. Chem. Geol. 291, 186−198.

Lott, D.A., Coveney, R.M., Murowchick, J.B., Grauch, R.I., 1999. Sedimentary exhalative nickel−molybdenum ores in South China. Econ. Geol. 94 (7), 1051−1066.

Lü, L.S., Mao, J.W., Li, H.B., Pirajno, F., Zhang, Z.H., Zhou, Z.H., 2011. Pyrrhotite Re−Os and SHRIMP zircon U−Pb dating of the Hongqiling Ni−Cu sulfide deposits in Northeast China. Ore Geol. Rev. 43 (1), 106−119.

Mao, J.W., Cheng, Y.B., Chen, M.H., Pirajno, F., 2013. Major types and time−space distribution of Mesozoic ore deposits in South China and their geodynamic settings. Miner. Deposita 48, 267−294.

Mao, J.W., Pirajno, F., Cook, N., 2011. Mesozoic metallogeny in East China and corresponding geodynamic settings − an introduction to the special issue. Ore Geol. Rev. 43 (1), 1−7.

Mao, J.W., Xie, G.Q., Guo, C.L., Yuan, S.D., Cheng, Y.B., Chen, Y.C., 2008. Spatial−temporal distribution of Mesozoic ore deposits in South China and their metallogenic settings. Geol. J. China Univ. 14, 510−526 (in Chinese with English abstract).

Marcantonio, F., Reisberg, L., Zindler, A., Wyman, D., Hulbert, L., 1994. An isotopic study of the Ni−Cu−PGE-rich Wellgreen intrusion of the Wrangellia Terrane: evidence for hydrothermal mobilization of rhenium and osmium. Geochim. Cosmochim. Acta 58 (2), 1007−1018.

Martin, C.E., 1991. Os isotopic characteristics of mantle derived rocks. Geochim. Cosmochim. Acta 55 (5), 1421−1434.

Mathur, R., Ruiz, J., Munizaga, F., 2000. Relationship between copper tonnage of Chilean base-metal porphyry deposits and Os isotope ratios. Geology 28 (6), 555−558.

Mathur, R., Ruiz, J., Tornos, F., 1999. Age and sources of the ore at Tharsis and Rio Tinto, Iberian pyrite belt, from Re−Os isotopes. Miner. Deposita 34 (8), 790−793.

Mathur, R., Titley, S., Ruiz, J., Gibbins, S., Friehauf, K., 2005. A Re−Os isotope study of sedimentary rocks and copper-gold ores from the Ertsberg District, West Papua, Indonesia. Ore Geol. Rev. 26 (3−4), 207−226.

McCandless, T.E., 1994. Evaluation of the Molybdenite Rhenium−osmium Geochronometer, and its Application to Base Metal Porphyry Mineralization. The University of Arizona, pp. 1−96.

McCandless, T.E., Ruiz, J., Campbell, A.R., 1993. Rhenium behavior in molybdenite in hypogene and near-surface environments: implication for Re–Os geochemistry. Geochim. Cosmochim. Acta 57 (4), 889–905.

Meisel, T., Walker, R.J., Morgant, J.W., 1996. The osmium isotopic composition of the Earth's primitive upper mantle. Nature 383 (10), 517–520.

Morgan, J.W., Wandless, G.A., Petrie, R.K., Irving, A.J., 1981. Composition of the earth's upper mantle-l. Siderophile trace elements in upper mantle Dodules. Tectonophysics 75 (1–2), 47–67.

Mu, Z.G., Zheng, S.H., Cao, Z.M., 1982. Hydrogen, oxygen and carbon isotope studies of the minerals and their fluid inclusion in the Shangbao pyrite deposit, Laiyang County, Hunan Province. Geol. Rev. 4, 367–369.

Munha, J., Kerrich, R., 1980. Sea water basalt interaction in spilites from the Iberian pyrite belt. Contrib. Mineral. Petrol. 73, 191–200.

Pasava, J., Hladikova, J., Dobes, P., 1996. Origin of Proterozoic metal-rich black shales from the Bohemian Massif, Czech Republic. Econ. Geol. 91, 63–79.

Pearson, D.G., Woodland, S.J., 2000. Solvent extraction/anion exchange separation and determination of PGEs (Os, Ir, Pt, Pd, Ru) and Re–Os isotopes in geological samples by isotope dilution ICP–MS. Chem. Geol. 165, 57–107.

Ravizza, G., Turekian, K.K., Hay, B.J., 1991. The geochemistry of rhenium and osmium in recent sediments from the Black Sea. Geochim. Cosmochim. Acta 55 (12), 3741–3752.

Ravizza, G., Turekian, K.K., 1992. The osmium isotopic composition of organic-rich marine sediments. Earth Planet. Sci. Lett. 110 (1–4), 1–6.

Ripley, E.M., Park, Y.R., Li, C., Naldrett, A.J., 1999. Sulfur and oxygen isotopic evidence for country rock contamination in the Voisey's Bay Ni–Cu–Co deposit, Labrador, Canada. Lithos 47, 53–68.

Selby, D., Creaser, R.A., 2001. Re–Os geochronology and systematics in molybdenite from the Endako porphyry molybdenum deposit, British Columbia, Canada. Econ. Geol. 96 (1), 197–204.

Selby, D., Kelley, K.D., Hitzman, M.W., Zieg, J., 2009. Re–Os sulfide (Bornite, Chalcopyrite, and Pyrite) systematics of the carbonate-hosted copper deposits at ruby Greek, southern Brooks range, Alaska. Econ. Geol. 104 (3), 437–444.

Sharma, M., Papanastassiou, D.A., Wasserburg, G.J., 1997. The concentration and isotopic composition of osmium in the oceans. Geochim. Cosmochim. Acta 61 (16), 3287–3299.

Shu, L.S., Jahn, B.M., Charvet, J., Santosh, M., Wang, B., Xu, X.S., Jiang, S.Y., 2014. Early Paleozoic depositional environment and intraplate tectono-magmatism in the Cathaysia Block(South China): new evidence for the Neoproterozoic breakup of Rodinia. Precambrian Res. 187 (3–4), 263–276.

Shu, X.J., Wang, X.L., Sun, T., Xu, X.S., Dai, M.N., 2011. Trace elements, U–Pb ages and Hf isotopes of zircons from Mesozoic granites in the western Nanling Range, South China: implications for petrogenesis and W–Sn mineralization. Lithos 127 (3–4), 468–482.

Smoliar, M.I., Walker, R.J., Morgan, J.W., 1996. Re–Os ages of group IIA, IIIA, IVA and IVB iron meteorites. Science 271, 1099–1102.

Snow, J.E., Reisberg, L., 1995. Os isotopic systematics of the MORB mantle: results from altered abyssal peridotites. Earth Planet. Sci. Lett. 133 (3–4), 411–421.

Stein, H.J., Markey, R.J., Morgan, J.W., Hannah, J.L., Schersten, A., 2001. The remarkable Re–Os chronometer in molybdenite: how and why it works. Terra Nova 13 (6), 479–486.

Stein, H.J., Sundblad, K., Markey, R.J., Morgan, G.B., Motuza, G., 1998. Re–Os ages for Archean molybdenite and pyrite, Kuittila-Kivisuo, Finland and Proterozoic molybdenite, Kabeliai, Lithuania testing the chronometer in a metamorphic and metasomatic setting. Miner. Deposita 33 (4), 329–345.

Sun, W.D., Yang, X.Y., Fan, W.M., Wu, F.Y., 2012. Mesozoic large scale magmatism and mineralization in South China: preface. Lithos 150, 1–5.

Sun, X.M., Wang, S.W., Sun, W.D., Shi, G.Y., Sun, Y.L., Xiong, D.X., Qu, W.J., Du, A.D., 2008. PGE geochemistry and Re–Os dating of massive sulfide ores from the Baimazhai Cu–Ni deposit, Yunnan province, China. Lithos 105 (1–2), 12–24.

Suzuki, K., Hiroshi, S., Akimasa, M., 1996. Re–Os dating of molybdenites from ore deposits in Japan implication for the closure temperature of the Re–Os system for molybdenite and the cooling history of molybdenum ore deposits. Geochim. Cosmochim. Acta 60 (16), 3151–3159.

Tu, D.F., 1984. Inclusions in minerals in the Shangbao pyrite district, Hunan. Geol. Rev. 8 (30), 270–274.

Volkening, J., Walczyk, T., Heumann, K.G., 1991. Osmium isotope ratio determinations by negative thermal ion mass spectrometry. Int. J. Mass Spect. Ion. Proc. 105, 147–159.

Walker, R.J., Morgan, J.W., 1989. Rhenium-osmium isotope systematics of carbonaceous chondrites. Science 243, 519–522.

Walker, R.J., Carlson, R.W., Shirey, S.B., Boyd, F.R., 1989. Os, Sr, Nd and Pb isotope systematics of southern African peridotite xenoliths: implications for the chemical evolution of subcontinental lithospheric mantle. Geochim. Cosmochim. Acta 53 (7), 1583–1595.

Walker, R.J., Morgan, J.W., Horan, M.F., Czamanske, G.K., Krogstad, E.J., Fedorenko, V.A., Kunilov, V.E., 1994. Re–Os isotopic evidence for an enriched-mantle source for the Noril'sk, ore-bearing intrusions, Siberia. Geochim. Cosmochim. Acta 58 (19), 4179–4197.

Walker, R.J., Morgan, J.W., Naldrett, A.J., Li, C., Fassett, J.D., 1991. Re–Os isotope systematics of Ni–Cu sulfide ores, Sudbury Igneous Complex, Ontario: evidence for a major crustal component. Earth Planet. Sci. Lett. 105, 416–429.

Walker, R.J., Shirey, S.B., Stecher, O., 1988. Comparative Re–Os, Sm–Nd and Rb–Sr isotope and trace element systematics for Archean komatiite flows from Munro Township, Abitibi Belt, Ontario. Earth Planet. Sci. Lett. 87, 1–12.

Wang, Y.J., Fan, W.M., Cawood, P.A., Ji, S.C., Peng, T.P., Chen, X.Y., 2007. Indosinian high-strain deformation for the Yunkaidashan tectonic belt, south China: kinematics and $^{40}Ar/^{39}Ar$ geochronological constraints. Tectonics 26 (6), 6008–6028.

Wang, Y.J., Fan, W.M., Cawood, P.A., Li, S.Z., 2008. Sr–Nd–Pb isotopic constraints on multiple mantle domains for Mesozoic mafic rocks beneath the South China Block hinterland. Lithos 106 (3–4), 297–308.

Wang, Y.J., Fan, W.M., Guo, F., Peng, T.P., Li, C.W., 2003. Geochemistry of Mesozoic mafic rocks adjacent to the Chenzhou-Linwu fault, South China: implications for the lithospheric boundary between the Yangtze and Cathaysia blocks. Int. Geol. Rev. 45 (3), 263–286.

Wang, Y.J., Zhang, A.M., Fan, W.M., Zhang, Y.H., Zhang, Y.Z., 2013. Origin of paleo-subduction-modified mantle for Silurian gabbro in the Cathaysia block: geochronological and geochemical evidence. Lithos 160–161, 37–54.

Wang, Y.J., Zhang, F.F., Fan, W.M., Zhang, G.W., Chen, S.Y., Cawood, P.A., Zhang, A.M., 2010. Tectonic setting of the South China Block in the early Paleozoic: resolving intracontinental and ocean closure models from detrital zircon U–Pb geochronology. Tectonics 29 (6), 6020–6035.

Xia, Y., Xu, X.S., Zou, H.B., Liu, L., 2014. Early Paleozoic crust–mantle interaction and lithosphere delamination in South China Block: evidence from geochronology, geochemistry, and Sr–Nd–Hf isotopes of granites. Lithos 184–187, 416–435.

Xu, X.S., O'Reilly, S.Y., Griffin, W.L., Wang, X.L., Pearson, N.J., He, Z.Y., 2007. The crust of Cathaysia: age, assembly and reworking of two terranes. Precambrian Res. 158 (1–2), 51–78.

Xu, X.S., Xie, X., 2005. Late Mesozoic–Cenozoic basaltic rocks and crust–mantle interaction, SE China. Geol. J. China Univ. 11 (3), 318–334 (in Chinese with English abstract).

Yao, W.H., Li, Z.X., Li, W.X., Wang, X.C., Li, X.H., Yang, J.H., 2012. Post-kinematic lithospheric delamination of the Wuyi–Yunkai orogen in South China: evidence from ca. 435 Ma high-Mg basalts. Lithos 154, 115–129.

Yu, Y., Huang, X.L., He, P.L., Li, J., 2016. I-type granitoids associated with the early Paleozoic intracontinental orogenic collapse along pre-existing block boundary in South China. Lithos 248–251, 353–365.

Zaw, K., Peters, S.G., Cromie, P., Burrett, C., Hou, Z.Q., 2007. Nature, diversity of deposit types and metallogenic relations of South China. Ore Geol. Rev. 31 (1–4), 3–47.

Zhang, L., Xiao, W., Qin, K., Qu, W., Du, A., 2005. Re–Os isotopic dating of molybdenite and pyrite in the Baishan Mo–Re deposit, eastern Tianshan, NW China, and its geological significance. Miner. Deposita 39 (8), 960–969.

Zhang, Q., Jiang, Y.H., Wang, G.C., Liu, Z., Ni, C.Y., Qing, L., 2015. Origin of Silurian gabbros and I-type granites in central Fujian, SE China: implications for the evolution of the early Paleozoic orogen of South China. Lithos 216–217, 285–297.

Zhou, X.M., Sun, T., Shen, W.Z., Shu, L.S., Niu, Y.L., 2006. Petrogenesis of Mesozoic granitoids and volcanic rocks in South China: a response to tectonic evolution. Episodes 29 (1), 26–33.